Nusselt number for flow perpendicular to arrays of cylinders in the limit of small Reynolds and large Peclet numbers

Wei Wang and Ashok S. Sangani

Related Articles

Bi-stability in turbulent, rotating spherical Couette flow
Phys. Fluids 23, 065104 (2011)

Turbulent mixing and passive scalar transport in shallow flows
Phys. Fluids 23, 016603 (2011)

Numerical simulation of reciprocating turbulent flow in a plane channel
Phys. Fluids 21, 095106 (2009)

Eigenmode analysis of scalar transport in distributive mixing
Phys. Fluids 21, 093601 (2009)

Decomposition driven interface evolution for layers of binary mixtures. II. Influence of convective transport on linear stability
Phys. Fluids 21, 062104 (2009)

Additional information on Phys. Fluids

Journal Homepage: http://pof.aip.org/

Journal Information: http://pof.aip.org/about/about_the_journal

Top downloads: http://pof.aip.org/features/most_downloaded

Information for Authors: http://pof.aip.org/authors

Nusselt number for flow perpendicular to arrays of cylinders in the limit of small Reynolds and large Peclet numbers

Wei Wang and Ashok S. Sangani
Department of Chemical Engineering and Materials Science, Syracuse University, Syracuse, New York 13244

The problem of determining the Nusselt number N, the nondimensional rate of heat or mass transfer, from an array of cylindrical particles to the surrounding fluid is examined in the limit of small Reynolds number Re and large Peclet number Pe. N in this limit can be determined from the details of flow in the immediate vicinity of the particles. These are determined accurately using a method of multipole expansions for both ordered and random arrays of cylinders. The results for $N/Pe^{1/3}$ are presented for the complete range of the area fraction of cylinders. The results of numerical simulations for random arrays are compared with those predicted using effective-medium approximations, and a good agreement between the two is found. A simple formula is given for relating the Nusselt number and the Darcy permeability of the arrays. Although the formula is obtained by fitting the results of numerical simulations for arrays of cylindrical particles, it is shown to yield a surprisingly accurate relationship between the two even for the arrays of spherical particles for which several known results exist in the literature suggesting thereby that this relationship may be relatively insensitive to the shape of the particles. © *1997 American Institute of Physics.* [S1070-6631(97)00606-5]

I. INTRODUCTION

We consider the problem of determining the rate of heat or mass transfer from particles to the surrounding fluid. Although considerable work has been done on the problem of transfer from a single particle, there are very few studies that treat rigorously the case of multiparticle systems. Sorensen and Stewart[1] used a collocation technique to determine the heat transfer rates in a cubic array of fixed spheres at small Reynolds number Re and finite Peclet number Pe. The results of numerical computations were supplemented with an asymptotic analysis for large Peclet numbers in a separate study.[2] Here, $Re = aU/\nu$ and $Pe = aU/D$, a being the radius of the particles, ν the kinematic viscosity of the fluid, U the superficial velocity of the fluid through the array, and D the mass or heat diffusivity—the latter being related to the thermal conductivity κ, density ρ, and specific heat c_p by $D = \kappa/(\rho c_p)$. Sangani and Acrivos[3] used a somewhat different collocation technique to determine the heat transfer rates in square and hexagonal arrays of infinitely long cylinders, while Acrivos *et al.*[4] examined the case of dilute random arrays of spherical particles. Both of these studies were concerned with the case of vanishingly small Re and small but finite Pe.

In the present study we shall be interested in the opposite limit of Pe, i.e., in the limit of large Pe, the Reynolds number being vanishingly small. Since the Peclet number is a product of the Reynolds number and the Prandtl number $\sigma = \nu/D$, the above conditions are usually satisfied when the Prandtl number is large. This situation is very common in mass transfer applications, e.g., in mass transfer across the walls of hollow membranes, but it could also occur in heat transfer applications involving viscous oils. Note that the Prandtl and Nusselt numbers in mass transfer applications are sometimes referred to as, respectively, the Schmidt and Sherwood numbers. In what follows we shall consider the heat transfer problem, but the results will be equally applicable to the mass transfer problem.

When $Pe \gg 1$, the heat transfer by convection dominates over that by conduction on a length scale comparable to a. Consequently, the temperature along most streamlines is constant. Near the surface of heated particles there exists a thermal boundary layer of $O(aPe^{-1/3})$ thickness in which the heat transfer by conduction as well as convection are comparable in magnitude and the temperature along a streamline is generally not constant. The net rate of heat transfer can then be determined from the analysis of this thermal boundary layer. Since this analysis depends only on the fluid stress in the immediate vicinity of the particles, the heat transfer rates in the large Pe limit can be determined rather easily if the velocity field near each particle is available. We have used the numerical technique described by Sangani and Yao[5] to determine this velocity field and the
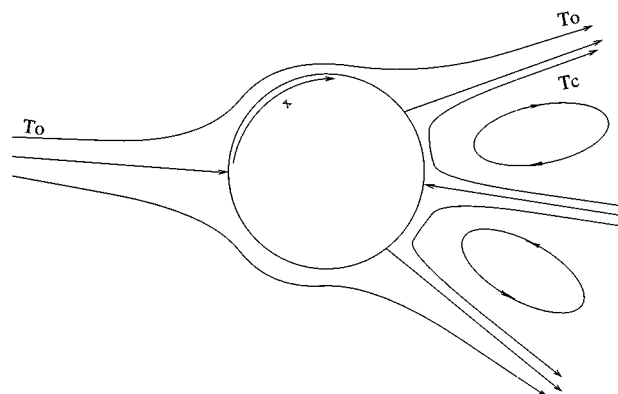

FIG. 1. A sketch of flow past a representative particle in a random array.

heat transfer rates from heated particles to the surrounding fluid. The results for the nondimensional heat transfer coefficient, Nusselt number N, are presented for both periodic and random arrays of cylinders. The results for random arrays compare well with those predicted by effective-medium approximations. A simple formula is given that accurately relates the Nusselt number to the Darcy permeability of the arrays for a wide range of volume fractions over which the permeability varies by several orders of magnitude. The formula is also shown to be surprisingly accurate even when applied to the arrays of spherical particles for which several known results exist in the literature.

II. THEORY

A. Role of open versus closed streamline regions

Before we begin with the detailed analysis of the problem, it is useful to discuss the role of open and closed streamline regions in determining the leading-order contributions to N in the limit of large Pe. It is well known from the studies of heat transfer from a single particle that N can vary significantly depending upon whether the flow in the immediate vicinity of a particle is a part of open streamlines or closed streamlines. Thus, for example, when the flow around a single particle is due to uniform streaming at infinity, which has no regions of closed streamlines, N increases as $Pe^{1/3}$ in the limit of large Pe,[6,7] while for a particle freely suspended in a shear flow, for which there exists a region of closed streamlines surrounding the whole particle, N approaches an $O(1)$ constant.[8,9] Since the flow around individual particles in a random array of cylinders can be quite complex and may include regions of closed streamlines, we must first determine if the heat transfer from the closed streamline region will be significant.

Let us consider then a flow around a representative particle in a fixed array. The flow is illustrated in Fig. 1 where we have assumed that there are several stagnation points along the surface of the particle and that some of these stagnation points arise from the regions of closed streamlines in the vicinity of the particle. Note that the number of stagnation points must be an even integer. We expect the temperature along each streamline to be constant in the limit $Pe \rightarrow \infty$ except in the thin thermal boundary layer regions. Let the temperature of the open streamline shown in Fig. 1 be T_o and that of a closed streamline in the immediate vicinity of the particle be T_c. The rate of heat transfer from the particle surface maintained at T_s to the fluid in the open streamline region will be proportional to $(T_s - T_o)Pe^{1/3}$, and that to the fluid in the closed streamline region will likewise be proportional to $(T_s - T_c)Pe^{1/3}$. The heat removed by the closed streamline must in turn be rejected into the open streamline region whose temperature, as mentioned above, is T_o. Since the boundary dividing the regions of open and closed streamlines is a free surface where the velocity is nonzero, and since the heat transfer rates across free surfaces increase as $Pe^{1/2}$ (see, for example, Leal[10]), the rate at which the heat is exchanged between the two regions is proportional to $(T_c - T_o)Pe^{1/2}$. Thus, at steady state we must have that
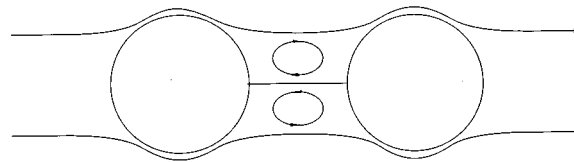

FIG. 2. A sketch of flow around two particles oriented in the direction of the flow. The heat transfer from the second particle is reduced due to the fact that the fluid in its contact is already heated by the first particle.

$$(T_c - T_o)Pe^{1/2} = \text{const} \ (T_s - T_c)Pe^{1/3}. \qquad (1)$$

In other words, $T_c - T_o = \text{const} \ (T_s - T_c)Pe^{-1/6}$, indicating thereby that to leading order the temperatures of the open as well as the closed streamlines in the immediate vicinity of the particle are equal and different from that of the particle surface.[11] As a consequence, we expect N to increase as $Pe^{1/3}$, with the next term in the expansion being $O(Pe^{1/6})$ in magnitude.

The above argument is based on two assumptions. The first is that the number of stagnation points around each particle is nonzero. If this number is zero for some particles, as is the case for the freely suspended particles in a simple shear flow, the rate of heat transfer from such particles will be $O(1)$ instead of $O(Pe^{1/3})$. The heat transfer contribution from such particles must be neglected since they will not contribute to the leading, $O(Pe^{1/3})$, term that is of interest to us in the present study.

The second assumption is that the open streamline coming close to the surface of the heated particle has not come in contact previously with another heated particle as in the case shown in Fig. 2. In this case the capacity to remove heat from the second particle is greatly reduced since the fluid near the surface of the second particle is already heated due to its contact with the first particle. This situation would occur in the case of a periodic array when the mean flow is along a principal lattice direction. Indeed, as pointed out by Sorensen and Stewart,[2] the thermal boundary layer would continue to grow in such a case and the thickness of the thermal boundary layer would eventually become comparable to the particle radius sufficiently downstream of the flow. Consequently, N would be $O(1)$ for far downstream regions of the array. The results we shall present here therefore apply only to heat transfer from a single active particle in a periodic array. It should be noted that this is a particularly severe restriction only in the case of periodic arrays. For random arrays it does not pose a serious restriction because the probability that a streamline emanating from a given heated particle will come in contact with another heated particle in its vicinity is small. Since the volume occupied by the fluid is proportional to $1 - \phi$, and that occupied by the thermal boundary layers near each particle is proportional to $\phi Pe^{-1/3}$, the probability that the heat removed from a heated particle and carried away along an outgoing streamline will be dispersed into the fluid is $(1 - \phi)Pe^{1/3}/\phi$ times greater than the probability that it will affect the boundary layer behavior of another particle. Thus N in random arrays will be $O(Pe^{1/3})$ even in the far downstream regions of the array. The situation described here is

analogous to that observed for heat transfer in tubes. The Nusselt number at large Pe is $O(1)$ at large distances into the tube when the flow is laminar, for which the same fluid elements continue to stay in contact with the heated tube walls, compared with N that scales approximately as $R^{0.8}$ when the flow is turbulent which continuously exposes the heated wall to fresh, unheated fluid from the bulk of the flow.

B. An expression for the Nusselt number

Since the thermal boundary layers are much thinner than the particle radii, it will suffice to consider the energy equation in its simplified form,

$$Y\tau_w\frac{\partial T}{\partial x}-\frac{1}{2}Y^2\tau_w'\frac{\partial T}{\partial Y}=\frac{\partial^2 T}{\partial Y^2}+O(Pe^{-1/3}), \tag{2}$$

where $Y=(r-1)Pe^{1/3}$ is the scaled distance normal to the surface of a representative particle, r being nondimensionalized by the particle radius a, x is the distance measured along the surface of the particle with $x=0$ representing an incoming stagnation point (defined as a point where the streamline is along the radial direction and pointing into the particle surface, cf. Fig. 1), T is the temperature of the fluid, $\tau_w\equiv\tau_w(x)=(\partial u/\partial r)_w$ is the radial derivative of the tangential component u of the velocity evaluated at the particle surface, and the prime denotes differentiation with respect to the argument of a function, e.g., $\tau_w'=d\tau_w/dx$. In writing (2) we have made use of the fact that for small distances from the particle surface the velocity components parallel and normal to the surface of the particle are approximately given by $\tau_w(x)(r-1)$ and $-\tau_w'(r-1)^2/2$, respectively.

The solution of (2) by the similarity transformation is relatively well known. Taking $T=T_o+(T_s-T_o)f(s)$ with $s=Y/g(x)$ and $Y=(r-1)Pe^{1/3}$ yields

$$f''+3s^2f'=0 \tag{3}$$

and

$$g^2g'\tau_w+\frac{1}{2}g^3\tau_w'=3, \tag{4}$$

together with the boundary conditions $f(0)=1$ and $f(\infty)=0$. The boundary condition for g will be discussed later. The solution for f is, of course, straightforward and given by

$$f=\frac{1}{\Gamma(4/3)}\int_s^\infty e^{-t^3}dt, \tag{5}$$

where $\Gamma(4/3)=0.892\,97\ldots$ is the gamma function of 4/3. Since (4) can be rewritten as $(g^3\tau_w^{3/2})'=9\tau_w^{1/2}$, we obtain, upon integrating,

$$g^3(x)=9\tau_w^{-3/2}(x)\int_0^x\tau_w^{1/2}(t)dt+A\tau_w^{-3/2}(x), \tag{6}$$

where A is a constant of integration. Now the usual argument for estimating A consists of requiring that g be finite at the incoming stagnation point ($x=0$). Since $\tau_w=0$ at $x=0$, this argument gives $A=0$. This result is correct provided that the incoming fluid at the stagnation point has not come in contact with the particle previously as is the case with the point
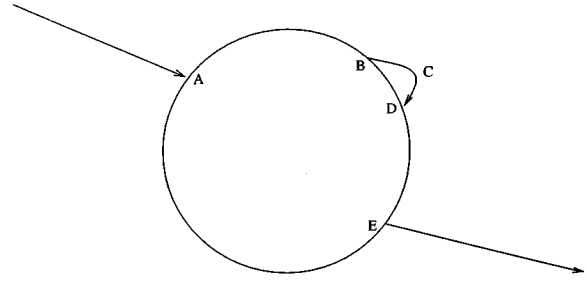

FIG. 3. A sketch illustrating detachment and reattachment of flow inducing a region of closed streamline. The heat lost by the particle along ABDE is carried away by the fluid leaving the particle at E.

D shown in Fig. 3. In the situation shown in Fig. 3, the fluid detaches at point B and reattaches at point D and hence the boundary layer thickness, which is proportional to g, at D is expected to be thicker than what it would have been if D were a stagnation point corresponding to fresh, unheated fluid. To obtain the proper conditions for determining A then, we must use the overall energy balance. Since all the heat lost $Q(x)$ by the particle up to some distance x from the stagnation point A must be equal to the net gain in the enthalpy of the fluid, we have that

$$Q(x)=\rho c_p Pe^{-1/3}\int_0^\infty u(T-T_o)dY, \tag{7}$$

where $u\equiv u(x,Y)$ and $T\equiv T(x,Y)$. Substituting $u=Y\tau_w(x)Pe^{-1/3}$ and $T-T_o=(T_s-T_o)f$, and performing the integration in the term on the right-hand side of the above equation, we obtain

$$\int_0^\infty u(T-T_o)dY=\frac{T_s-T_0}{6Pe^{1/3}\Gamma(4/3)}g^2\tau_w(x). \tag{8}$$

Substituting in (7) we have

$$g^2\tau_w(x)=\frac{6Pe^{2/3}\Gamma(4/3)Q(x)}{\rho c_p(T_s-T_o)}. \tag{9}$$

Now, rewriting (6) as

$$g^2\tau_w(x)=\left[9\int_0^x\tau_w^{1/2}(t)dt+A\right]^{2/3} \tag{10}$$

and comparing it with (9), we see that A can be related to the heat gained by the fluid up to a given stagnation point. Thus we find that one must take $A=0$ to determine g along the arc AB in Fig. 3, but not along the arc DB or DE. Let Q_{AB}, Q_{DB}, and Q_{DE} be the rate of heat transfer along the arcs AB, DB, and DE, respectively. The heat Q_{DB} gained by the recirculating fluid along DB is rejected and hence gained by the fluid just outside the recirculating region along the arc BCD. As a result, the fluid approaching the point D from the open region has gained a total heat equal to $Q_{AB}+Q_{DB}$, and consequently,

$$A^{2/3}=\frac{6\Gamma(4/3)Pe^{2/3}(Q_{AB}+Q_{DB})}{\rho c_p(T_s-T_o)} \tag{11}$$

for determining g along DE. Likewise, in determining g along DB we must use

$$A^{2/3} = \frac{6\Gamma(4/3) Pe^{2/3} Q_{AB}}{\rho c_p (T_s - T_o)}. \qquad (12)$$

It may be noted that g is not symmetric around all incoming stagnation points. For points such as A, the thermal boundary layer thickness on either side of the stagnation point is the same, while for the reattachment points such as D the thermal boundary layer thickness on the recirculation side is thinner than that on the open streamline side. Finally, it should also be noted that while the thermal boundary layer thickness increases along the arc BCD on the open streamline side, that on the closed streamline side decreases as a result of the heat transfer across BCD.

Now it is easy to show that the net rate of heat transfer per unit depth of a representative cylinder α is given by

$$Q^{\alpha} = \frac{3}{2} \frac{1}{9^{1/3} \Gamma(4/3)} \kappa a (T_s^{\alpha} - T_o) Pe^{1/3}$$

$$\times \sum_i \left\{ \int_0^{L_i} |\tau_w|^{1/2}(x) dx \right\}^{2/3}, \qquad (13)$$

where T_s^{α} is the temperature of particle α. The summation index i in the above expression refers to the ith pair of adjacent incoming-outgoing stagnation points (e.g., points A and E in Fig. 3), and L_i is the arc length between the two stagnation points normalized by the particle radius. Note that the stagnation points such as B and D are not to be considered as the incoming or outgoing stagnation points. The above expression is in agreement with that given by Sorensen and Stewart,[2] who, as mentioned earlier, considered the case of heat transfer in periodic arrays of spheres at large Pe. Note, however, that these investigators made no mention of the possibility that there may be more than two stagnation points per particle and that the stagnation points corresponding to regions of closed streamlines must be treated differently than the other stagnation points.

Now the Nusselt number in an array containing N_p particles (per unit cell) is defined as

$$N = \frac{1}{N_p} \sum_{\alpha=1}^{N_p} \frac{Q^{\alpha}}{2\pi a \kappa (\langle T_s \rangle - \langle T_f \rangle)}, \qquad (14)$$

where $\langle T_s \rangle$ and $\langle T_f \rangle$ are the average solid and fluid temperatures. The average temperature in the fluid phase may be defined in several ways, the two most common choices being the spatial average of the fluid temperature and the fluid velocity weighted average temperature, the so-called mixing-cup temperature. In the limit $Pe \to \infty$ both temperatures become equivalent and equal to T_o with an error of $O(Pe^{-1/6})$ occurring from the temperature in the closed streamline being different from that in the open streamline region.

Even though there is no ambiguity in defining $\langle T_f \rangle$, we should note that two different values of N are possible, depending upon whether we specify Q^{α} among all the particles to be the same or specify T_s^{α} to be the same for all particles. Let N_Q and N_T be the Nusselt numbers corresponding to

these two different situations. It is easy to show that, in the limit $Pe \to \infty$, $N_T \leq N_Q$ with the equality sign valid for periodic arrays, i.e., $N_p = 1$. In the extreme case, where some of the particles have no stagnation points, N_Q will be $O(1)$ even though N_T remains $O(Pe^{1/3})$.

C. The numerical method

From the preceding discussion we see that to determine the Nusselt numbers we need to determine the stagnation points and τ_w for each cylinder. We used the method of multipole expansion outlined in Sangani and Yao[5] for this purpose. The streamfunction ψ expressed in terms of a polar coordinate system with its origin at the center of particle α is given by

$$\psi = \sum_{n=0}^{\infty} h_n^{\alpha}(r) \cos n\theta + \tilde{h}_n^{\alpha}(r) \sin n\theta, \qquad (15)$$

where r and θ are defined by $x_1 - x_1^{\alpha} = r \cos \theta$ and $x_2 - x_2^{\alpha} = r \sin \theta$, $(x_1^{\alpha}, x_2^{\alpha})$ being the coordinates of the center of particle α, $\tilde{h}_0^{\alpha}(r) \equiv 0$, and

$$h_n^{\alpha}(r) = \begin{cases} C_0^{\alpha} \ln r + E_0^{\alpha} + F_0^{\alpha} r^2, & n=0 \\ C_1^{\alpha} r^{-1} + D_1^{\alpha}(r \ln r - r/2) + E_1^{\alpha} r + F_1^{\alpha} r^3, & n=1 \\ C_n^{\alpha} r^{-n} + D_n^{\alpha} r^{2-n} + E_n^{\alpha} r^n + F_n^{\alpha} r^{n+2}, & n \geq 2. \end{cases}$$
$$(16)$$

Similar relations hold for $\tilde{h}_n^{\alpha}(r)$. The no-slip boundary condition at $r=1$ gives

$$h_n^{\alpha}(1) = h_n^{\alpha'}(1) = \tilde{h}_n^{\alpha}(1) = \tilde{h}_n^{\alpha'}(1) = 0 \qquad (17)$$

except for $h_0(1)$, which equals the value of streamfunction at the surface of the particle. The method of multipole expansion is outlined in detail in Sangani and Yao.[5] In this method, ψ at any point in the fluid is expressed in terms of derivatives of periodic singular solutions of biharmonic equations. The coefficients of these derivatives are directly related to the coefficients of the singular terms in (16), i.e., to C_n^{α}, D_n^{α}, $\tilde{C}_n^{\alpha}$, and $\tilde{D}_n^{\alpha}$. When the summation in (15) is truncated to $n \leq N_s$, these represent a total of $(4N_s + 1) N_p$ unknowns in this global expansion of ψ. The coefficients of the regular terms, i.e., E_n^{α}, F_n^{α}, etc. in the local expansion (15) and (16) near each particle are related to nth-order derivatives of the regular part of ψ at $\mathbf{x} = \mathbf{x}^{\alpha}$ and can therefore be expressed in terms of coefficients C_n^{α}, etc., through the global expansion of ψ. Application of (17) for $n \leq N_s$ then gives a total of $(4N_s + 1) N_p$ linear equations in the same number of unknowns. These equations are solved numerically to determine C_n^{α}, D_n^{α}, $\tilde{C}_n^{\alpha}$, and $\tilde{D}_n^{\alpha}$. The coefficients of the regular terms in (16) are subsequently determined using (17).

Now since the tangential component of the velocity is given by $u_{\theta} = -\partial\psi/\partial r$, τ_w is evaluated using

$$\tau_w = \pm \left(\frac{\partial u_\theta}{\partial r} \right)_{r=1}$$

$$= \pm \sum_{n=0}^{\infty} \left[\left(\frac{d^2 h_n^\alpha}{dr^2} \right)_{r=1} \cos n\theta + \left(\frac{d^2 \tilde{h}_n^\alpha}{dr^2} \right)_{r=1} \sin n\theta \right]. \quad (18)$$

The plus sign must be used in the term on the extreme right-hand side of the above expression when the curve joining an incoming stagnation point to an outgoing stagnation point is along the direction of decreasing θ.

The stagnation points on the surface of particle α are determined by solving $\tau_w(\theta) = 0$. The zeros of τ_w were determined by evaluating τ_w in small increments of θ and by using linear interpolation between two successive values of θ for which τ_w changed its sign. Now, to determine the Nusselt number we need to differentiate between those stagnation points where either the fresh unheated fluid comes in contact with the particle or the heated fluid leaves the particle and those stagnation points corresponding to the regions of closed streamlines. This is done by a two-step procedure.

First, we determine whether a given pair of stagnation points lies in the open streamline region or the closed streamline region using the following criteria: (1) If the arc length between the two stagnation points is greater than $\pi/3$ we treat the pair as corresponding to an open region because it is very unlikely that closed streamline regions greater than this arc length would form around a particle; (2) for pairs with arc length less than $\pi/3$ we estimate an approximate radial distance δ from the surface of the particle at which the tangential component of the velocity changes its sign for a value of θ exactly halfway between the two stagnation points. δ is estimated by assuming that u_θ is adequately given by the first two terms in the Taylor series expansion:

$$u_\theta(r) = -(r-1) \frac{\partial^2 \psi}{\partial r^2}(1) - \frac{(r-1)^2}{2} \frac{\partial^3 \psi}{\partial r^3}(1). \quad (19)$$

The above expansion yields $\delta = -2(\partial_{rr}\psi / \partial_{rrr}\psi)$ where ∂_r stands for a partial derivative with respect to r. The pair of stagnation points was regarded as corresponding to a closed streamline region provided that $0 < \delta < 0.2$.

Once each pair of stagnation points was labeled as corresponding to either a closed or an open streamline region, the next task is to determine the stagnation points such as A and E in Fig. 3 where either the fresh fluid enters or the heated fluid leaves the particle. We shall refer to these as "open" stagnation points. We used the following procedure to identify them: (1) If a stagnation point is surrounded on either side by open streamline regions, then that point is labeled as an "open" stagnation point; (2) if fewer than two stagnation points meet this criterion for a given particle, then we must have situations such as those sketched in Fig. 4. In such cases we choose the stagnation point with an equal number of closed streamline regions around it as an "open" stagnation point. This procedure will label A and B as the "open" stagnation points for the situations sketched in Fig. 4. This is a somewhat arbitrary procedure, but it is at least appropriate for the case of periodic arrays with the mean flow along a principal lattice direction. For most cases in-
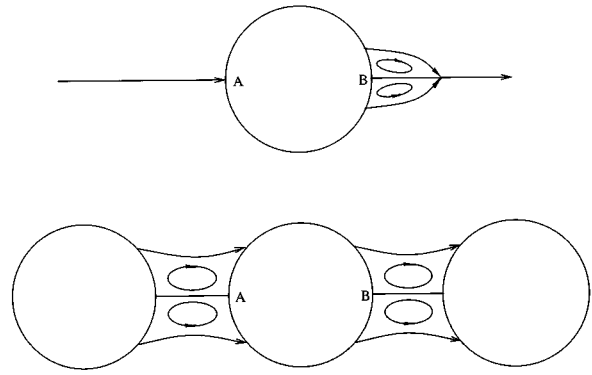

FIG. 4. Two representative situations for which the choice of "open" stagnation points is not obvious. The points indicated by A and B were chosen as the "open" stagnation points in such situations.

volving either oblique flows in periodic arrays or for random arrays the second scenario occurred with much less frequency and therefore we believe that this somewhat arbitrary scheme used in determining the "open" stagnation points will not affect significantly the results to be presented in the next section.

Q^α was determined by evaluating the integral in (13) over all pairs of "open" stagnation points using Simpson's rule. N_T was determined by averaging Q^α over all the particles in the array while N_Q was determined by taking the harmonic mean of Q^α over all the particles, $T_s - T_o$ being taken to be unity in both cases. In what follows we shall present results for the coefficients of $O(Pe^{1/3})$ in the expression for the Nusselt numbers,

$$N_{Q,T} = C_{Q,T} Pe^{1/3} + O(Pe^{1/6}), \quad (20)$$

and the coefficient of Darcy permeability,

$$K \equiv \frac{k}{a^2} = \frac{\pi \mu \langle u \rangle}{\phi \langle F \rangle}. \quad (21)$$

Here, k is the Darcy permeability of the array, μ is the fluid viscosity, $\langle u \rangle$ is the superficial velocity, ϕ is the area fraction of cylinders, and $\langle F \rangle$ is the average drag force per unit length of cylinders.

III. RESULTS

A. Periodic arrays

We first present results for periodic arrays in which the centers of the cylinders coincide with a square lattice, which corresponds to $N_p = 1$. The permeability is independent of the orientation θ_0 of the mean flow with respect to the principal lattice direction aligned along the x_1 axis. This, however, is not the case with N which is a function of θ_0. In this rather specialized geometry one must also be concerned about the fact that if $\tan \theta_0$ is a rational number then the cylinders sufficiently downstream of the flow will always be in a thermal wake of cylinders ahead of it. As mentioned earlier, the thermal boundary layers on the downstream

TABLE I. Convergence of numerical results for permeability and Nusselt number for square arrays of cylinders.

ϕ	Orientation	N_s	K	C	$C\phi^{1/3}K^{1/3}$	N_{stag}
0.01	0°	9	39.36	0.50	0.36	2
0.1	0°	5	1.27	0.68	0.34	2
		9	1.27	0.68	0.34	2
0.1	45°	5	1.27	0.72	0.36	2
		9	1.27	0.72	0.36	2
0.5	0°	5	1.18E-2	1.27	0.23	6
		9	1.18E-2	1.27	0.23	6
		15	1.18E-2	1.27	0.23	6
0.5	45°	5	1.18E-2	1.59	0.29	2
		9	1.18E-2	1.59	0.29	2
		15	1.18E-2	1.59	0.29	2
0.7	0°	9	3.44E-4	2.38	0.15	10
		19	3.32E-4	2.26	0.14	14
		23	3.32E-4	2.26	0.14	18
0.7	10°	19	3.32E-4	2.69	0.17	2
		27	3.32E-4	2.69	0.17	2
0.7	45°	19	3.32E-4	3.00	0.18	2
		27	3.32E-4	3.00	0.19	2

TABLE II. Results for K and C for square arrays of cylinders at various ϕ and mean flow orientations.

ϕ	K	C			
		0°	15°	30°	45°
0.01	39.96	0.50	0.50	0.50	0.50
0.05	15.56	0.60	0.61	0.62	0.62
0.10	1.27	0.68	0.70	0.71	0.72
0.20	0.30	0.80	0.85	0.88	0.90
0.30	0.10	0.91	1.02	1.06	1.08
0.40	3.60E-1	1.06	1.22	1.28	1.30
0.50	1.18E-2	1.27	1.49	1.57	1.59
0.60	2.97E-2	1.57	1.90	2.01	2.05
0.70	3.32E-3	2.72	2.79	2.95	3.00

heated cylinders will become comparable to the particle radius and, consequently, N for such particles will be $O(1)$. The results presented here will therefore apply only to either the first row of cylinders or to the heat or mass transfer from a single active particle in a periodic array.

Table I shows the convergence of $K \equiv (k/a^2)$ and C as a function of N_s for several different values of the orientation angle θ_0 and the cylinder area fraction ϕ. The resistance to flow increases and hence K decreases as ϕ increases. Similarly, one expects the Nusselt number, and hence C, to increase with ϕ. The results for the permeability are in perfect agreement with those obtained using a boundary collocation method by Sangani and Acrivos.[3] We see that in general there is a rapid convergence of both K and C with N_s. Also shown in the table are the total number of stagnation points N_{stag} (including the closed as well as open stagnation points) for various values of θ_0. We found $N_{\text{stag}}=2$ for most values of θ_0, except for θ_0 close to 0. Interestingly, at $\phi=0.7$ and $\theta_0=0°$, we found N_{stag} to be as high as 18. The number of "open" stagnation points was 2 in all the cases considered here, and the procedure outlined above for determining the open stagnation points ensured that the Nusselt number varied smoothly as θ_0 is varied even though the total number of stagnation points varied abruptly from as high as 18 to 2 for some values of θ_0 and ϕ. The fact that the total number of stagnation points in the square arrays of cylinders is very sensitive to the orientation of the mean flow has been noted earlier by Larson and Higdon.[12] These investigators have illustrated the changes in the flow field through detailed streamline plots. In particular, their streamline plots at area fraction of 0.4 clearly show six stagnation points when the mean flow is almost parallel to one of the principal lattice directions and two stagnation points otherwise. This is in agreement with our calculations for the number of stagnation

points as a function of the orientation of the mean flow.

Since τ_w scales approximately linearly with the total drag force experienced by a particle, and since the drag force is proportional to $1/(\phi K)$, we expect $C\phi^{1/3}K^{1/3}$ to remain approximately constant over a wide range of ϕ values. This is confirmed by the results shown in Table I where $C\phi^{1/3}K^{1/3}$ is seen to vary only by a factor of about 2 as ϕ is varied from 0.01 to 0.7. The corresponding changes in ϕK and C are by factors of 10^4 and 5, respectively. It is easy to show from the analysis of a thermal boundary layer around a single cylinder that $C\phi^{1/3}K^{1/3}$ should approach 0.365 as $\phi \to 0$. This is in reasonable agreement with the results of numerical simulations shown in Table I.

Table II gives the detailed results for C as a function of ϕ for selected values of θ_0. These results for square arrays of cylinders are also shown in Fig. 5. We see that C, and hence the Nusselt number, increases monotonically with θ_0 as the latter is varied from 0° to 45°.

B. Random arrays

Results for random arrays are shown in Table III and Figs. 6 and 7. The random configurations of hard disks were
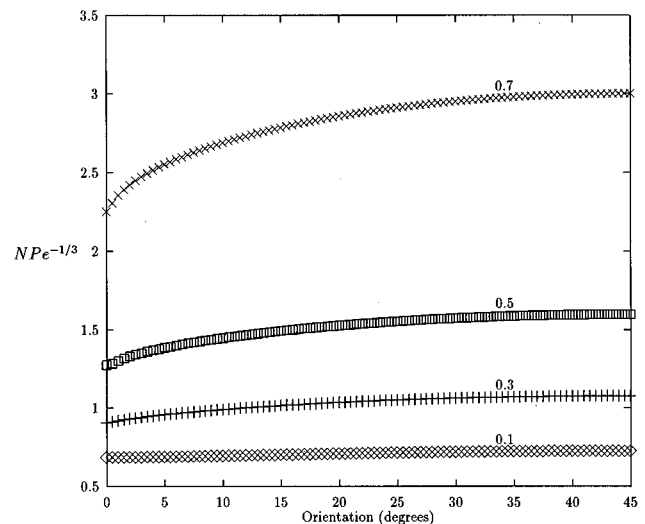

FIG. 5. Nusselt number as a function of the orientation of mean flow for various area fractions ϕ of cylinders.

TABLE III. Results for hard-disk, random configurations. K is the permeability coefficient computed in the present study while K_{SM}, K_{KL}, and K_G represent the results for the same obtained by, respectively, Sangani and Mo (Ref. 13), Koch and Ladd (Ref. 14), and Ghaddar (Ref. 12). K_{SQ} represents the permeability of square arrays of cylinders obtained by Sangani and Acrivos (Ref. 3). C_Q and C_T are the coefficients of the leading, $O(Pe^{1/3})$, term in the Nusselt number and N_{stag} is the average number of stagnation points per cylinder.

ϕ	N_p	N_s	K	K_{SM}	K_{KL}	K_G	K_{SQ}	C_T	C_Q	N_{stag}
0.05	64	7	5.64		5.63	3.89	4.01	0.53	0.53	2.14
0.1	64	9	1.70	1.67	1.68	1.45	1.27	0.60	0.59	2.23
0.3	64	9	8.94E-2	9.33E-2	1.08E-1	9.70E-2	1.02E-1	0.95	0.93	2.43
0.5	64	10	7.49E-3	8.28E-3	9.56E-3	7.87E-3	1.18E-2	1.50	1.40	2.77
0.6	49	11	1.85E-3	1.90E-3	1.87E-3		2.97E-3	1.83	1.75	3.57

generated by a usual molecular dynamics code. The results shown were obtained by averaging over 20 independent hard-disk configurations for each ϕ. For $\phi=0.5$ and 0.6 we started from a square array of cylinders with random initial velocities and allowed roughly 10^4 collisions per particle before selecting the arrays for computations. For smaller values of ϕ, the particles were given initially nonoverlapping random positions and velocities and were allowed to undergo about 5000 collisions per particle before selecting arrays for computations. The computations were made using a single IBM SP2 processor, and since the equations were solved using an $O(N^3)$ algorithm we limited calculations to moderate values of N_s as indicated in Table III. Convergence tests with few representative configurations for each ϕ indicated that the chosen values of N_s were adequate for determining permeability and the Nusselt number within about 10% accuracy.

Unlike the case of square arrays, we expect that N will depend on whether the flux from each particle or the temperature of the particle is specified. The results are presented for both C_Q and C_T. We note that the difference between the two is relatively small for all values of ϕ. Also shown in the table are the results for K, the permeability coefficient, and N_{stag}, the average number of total stagnation points per cylinder, as a function of ϕ. The average permeability coefficient was determined by first determining the average force exerted on cylinders over all the configurations and then using $K=\pi\mu U/\phi\langle F\rangle$, U being unity for all the configurations. Note that this will usually give estimates of K that are different from those obtained by fixing the net pressure drop across the array and determining the average of U among all the configurations, as has been done, for example, by Ghaddar.[13]

We first discuss the results for K. Table III shows a comparison with the results obtained by previous investigators. Sangani and Mo[14] used a low-order multipole expansion ($N_s=2$), but explicitly accounted for lubrication effects between pairs of particles. Here, by lubrication effects we mean the large pressure drop that occurs in the fluid as it moves through a narrow gap between a pair of particles. We see that there is generally good agreement between the results obtained by that method and with those obtained in the present study, with a notable difference occurring only for $\phi=0.5$. Ghaddar[13] used a finite element technique to determine K. He kept the unit cell size approximately constant and varied ϕ and N_p. Thus, for example, he used only $N_p=3$ for $\phi=0.05$. As a result, his results for low ϕ deviate significantly from the results obtained here. For reference,
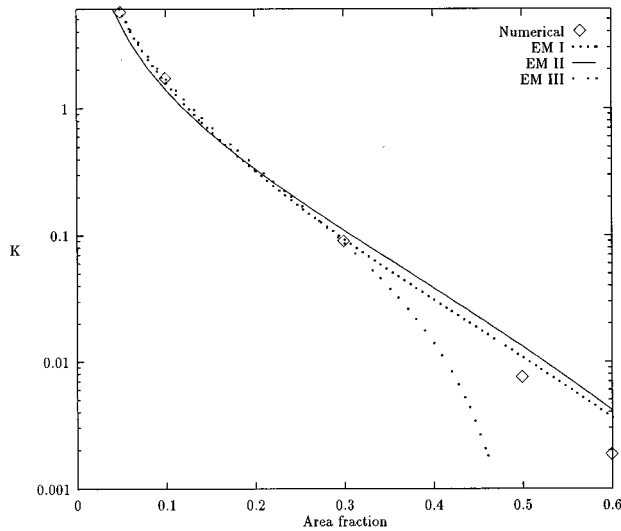

FIG. 6. A comparison of various effective medium-approximations and the computed values of the permeability coefficient K for the random arrays of cylinders.
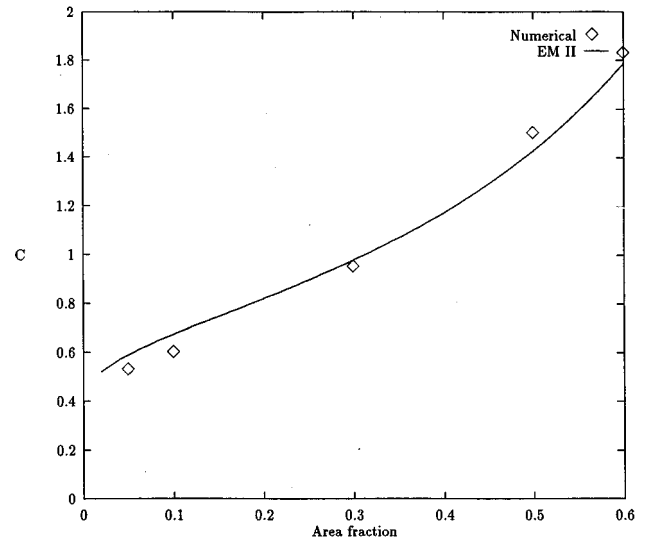

FIG. 7. A comparison of the effective-medium approximations and the computed values of the $O(Pe^{-1/3})$ coefficient C.

Phys. Fluids, Vol. 9, No. 6, June 1997

W. Wang and A. S. Sangani   1535

we have also tabulated K for square arrays of cylinders which correspond to $N_p = 1$. It may be noted that K determined by Ghaddar for $\phi = 0.05$ is closer to the result for square arrays than for random arrays. Koch and Ladd[15] used a lattice-Boltzmann technique for determining K. These investigators used $N_p = 64$ for smaller ϕ and $N_p = 32$ for $\phi = 0.5$ and 0.6. They obtained their results by averaging over ten configurations at smaller ϕ and five for larger ϕ. We see a very good agreement between our results and the results obtained by these investigators, except for $\phi = 0.5$; the reason for the observed discrepancy at this ϕ is unknown to us.

Also shown in Table III are the results for the coefficients of the $O(Pe^{1/3})$ term in the Nusselt number. As mentioned earlier, we expect C_T, the coefficient based on an assumption of same T for all the particles, to be greater than C_Q, the coefficient based on same heat flux for all the particles. The difference, however, is small at all ϕ. As in the case of square arrays, we see that C_T or C_Q increases with ϕ.

Finally, Table III also shows the average number of stagnation points per particle in random arrays. We did not observe a single case in which any of the particles was completely surrounded by the region of closed streamlines. Thus we conclude that all particles contribute significantly to the overall heat transfer coefficient. It is interesting to note that the maximum in average N_{stag}, which occurs at $\phi = 0.6$, is only 3.5, indicating that there are far fewer regions of closed streamlines in random arrays than observed in square arrays with the mean flow oriented along the principal lattice direction.

C. Comparison with approximate methods

It is interesting to compare the results obtained here with those predicted by approximate methods. There are, of course, numerous *ad hoc* methods and we shall not attempt to cover them all. Instead, we have chosen two methods for detailed comparison. The first is based on the effective-medium approximation while the second is based on a concept of hydraulic diameter commonly used in the design of heat exchangers.

The effective-medium approximations attempt to estimate various properties by analyzing a model system in which a particle of radius a is surrounded by fluid up to a radius aR and an effective-medium beyond it. Different effective-medium theories vary in their choices of R, the most popular choices being $R = \phi^{-1/2}$ and $R = 1$. Recently, Dodd *et al.*[16] determined various hydrodynamic coefficients (self- and collective translational and rotational mobilities) for random arrays of cylinders and found that the results of numerical simulations were generally in good agreement with an effective-medium theory in which R was defined in terms of a zero-wave-number structure factor of the array:

$$R^2 = \frac{1 - S(0)}{\phi}. \tag{22}$$

The structure factor is defined by

$$S(0) = n \int [g(\mathbf{r}|\mathbf{0}) - 1] dV_{\mathbf{r}}, \tag{23}$$

where $n = \phi/(\pi a^2)$ is the number density of particles and $ng(\mathbf{r}|\mathbf{0})$ is the pair probability density, i.e., probability of finding a particle with its center in the vicinity of $\mathbf{r}$ given that a particle is present at the origin. Note that ng equals a delta function at $r = 0$ and that $g \to 1$ as $r \to \infty$. The rationale for choosing R based on (22) may be found in Dodd *et al.*[16] and Mo and Sangani,[17] where it is shown that the conditionally averaged velocity field far from a given particle in sedimenting suspensions is correctly represented when R is defined by (22). For random, hard-disk systems $S(0)$ is given by Chae *et al.*:[18]

$$S(0) = \frac{(1 - 1.9682\phi + 0.9716\phi^2)^2}{1 + 0.0636\phi - 0.5446\phi^2 - 0.4632\phi^3 - 0.1060\phi^4 + 0.0087\phi^5}. \tag{24}$$

It should be noted that $S(0) \to 1 - 4\phi$ as $\phi \to 0$ so that $R \to 2$ as $\phi \to 0$. According to this model then the effective-medium in very dilute arrays extends beyond $R = 2$ as compared with $R = \phi^{-1/2} \to \infty$ in the usual effective-medium approximation. Thus one expects that, at least for dilute random arrays, the estimates based on (22) will be more accurate than those based on $R = \phi^{-1/2}$. This was indeed shown to be the case in the calculations of (1) the hydrodynamic mobilities;[16] (2) the diffusion-controlled reaction rates in arrays of cylinders;[19] and (3) the effective elastic properties of composite materials containing spherical inclusions.[20] Thus it is natural to inquire if this simple model also gives reasonably accurate estimates of K and N.

To obtain effective-medium estimates of N and K we

solve the following problem for the conditionally averaged velocity field $\mathbf{u}$:

$$\mu \nabla^2 \mathbf{u} = \nabla p, \quad \nabla \cdot \mathbf{u} = 0, \quad a < r < aR, \tag{25}$$

$$\mu \nabla^2 \mathbf{u} = \nabla p + \alpha^2 \mu \mathbf{u}, \quad \nabla \cdot \mathbf{u} = 0, \quad r > aR. \tag{26}$$

Thus the fluid motion satisfies the Stokes equations for $r < aR$ and Brinkman's equations for $r > aR$. The Brinkman viscosity is taken to be the same as the fluid viscosity. α^2 is the inverse of permeability to be determined as a part of the solution. The numerical scheme for determining α^2, and hence k, then consists of solving (25) and (26) subject to boundary conditions $\mathbf{u} = 0$ at $r = a$ and $\mathbf{u} = \mathbf{U}$ as $r \to \infty$ for an assumed value of α, the velocity and traction being continu-

TABLE IV. Comparison with the predictions of effective-medium approximations: EM I, EM II, and EM III correspond, respectively, to $R^2 = [1 - S(0)]/\phi$, $R^2 = 1/\phi$, and $R = 1$. The results of numerical simulations are denoted by Ex.

	K				C			$C\phi^{1/3}K^{1/3}$		
ϕ	Ex	EM I	EM II	EM III	Ex	EM I	EM II	Ex	EM I	EM II
0.05	5.64	5.36	4.48	5.54	0.53	0.55	0.59	0.35	0.36	0.36
0.1	1.70	1.57	1.41	1.68	0.60	0.64	0.67	0.35	0.34	0.35
0.3	8.94E-2	9.21E-2	1.10E-1	8.58E-2	0.95	1.00	0.98	0.28	0.30	0.31
0.5	7.49E-3	1.07E-2	1.32E-2	-ve	1.50	1.49	1.43	0.23	0.26	0.27
0.6	1.85E-3	3.58E-3	4.13E-3	-ve	1.83	1.84	1.79	0.19	0.24	0.24

ous at $r = aR$. Once the velocity field is evaluated, the force **F** on the particle is evaluated and a new estimate of α is obtained from

$$\alpha^2 a^2 = \frac{\phi F}{\pi \mu U}. \tag{27}$$

This process is repeated until the results for F and α converge to desired accuracy.

Taking **U** to be a unit vector along the x_1 axis and a equal to unity, and expressing the velocity in terms of streamfunction ψ, we have for $1 < r < R$,

$$\psi = [Er + Fr^3 + D(r\log r - r/2) + Gr^{-1}]\sin\theta. \tag{28}$$

The no-slip boundary condition at $r = 1$ gives $E = -2G + D$ and $F = G - D/2$. The force on the particle, and hence α, is related to D by $\alpha^2 = 4\phi D$. Now the wall stress function is evaluated from

$$\tau_w = -\left(\frac{\partial u_\theta}{\partial r}\right)_{r=1} = \left(\frac{\partial^2 \psi}{\partial r^2}\right)_{r=1} = (8C - 2D)\sin\theta. \tag{29}$$

Substituting in (14) we obtain

$$N = \frac{6^{1/3}}{2\pi\Gamma(4/3)}\left(\int_0^\pi (\sin\theta)^{1/2}d\theta\right)^{2/3} D^{1/3}\left(\frac{4G}{D} - 1\right)^{1/3} Pe^{1/3}$$

$$= 0.58 D^{1/3}\left(\frac{4G}{D} - 1\right)^{1/3} Pe^{1/3}. \tag{30}$$

The above result can be expressed in terms of K by making use of (27) and relations $F = 4\pi\mu D$ and $K = 1/(\alpha^2 a^2)$ to obtain

$$N = 0.365(\phi K)^{-1/3}\left(\frac{4G}{D} - 1\right)^{1/3} Pe^{1/3}. \tag{31}$$

Table IV shows a comparison between the results of numerical predictions and the effective-medium approximations. We have chosen three different values of R: $R^2 = [1 - S(0)]/\phi$; $R^2 = 1/\phi$; and $R = 1$. These are referred to as, respectively, the EM I, EM II, and EM III approximations. This comparison is also shown in Fig. 6. We see that K is best approximated by EM III at low ϕ, but this approximation gives unrealistic negative values for ϕ greater than about 0.4. The EM I approximation, on the other hand, is reasonably accurate at small ϕ and remains positive for the complete range of ϕ. It also gives a better estimate than EM II for the whole range of ϕ. Considering that it only gives an error by at most a factor of 2 as ϕK varies by four orders of

magnitude, it should be regarded as reasonably accurate. Also shown in Table IV and Fig. 7 are the comparisons for the coefficient C of the leading $O(Pe^{1/3})$ term in N and for $C(\phi K)^{1/3}$. We have taken $C = C_T$. We see that the effective-medium approximations give very good estimates for C, with the maximum error for the EM I approximation being only about 6%. The coefficient $C(\phi K)^{1/3}$ is proportional to $(4G/D - 1)^{1/3}$ in (31). We see that EM I and EM II give approximately the same estimate for this quantity, and hence the difference in the estimates of C from these approximations arises due to different estimates of K.

It is also interesting to compare the results for C obtained here with those predicted by the correlations for Nusselt numbers in heat exchangers available in the standard heat transfer textbooks. For example, Welty et al.[21] suggest the following procedure based on a concept of equivalent hydraulic radius. First, N for flow transverse to a single cylinder is estimated from

$$N = 0.623 Pe^{1/3} \tag{32}$$

for $0.2 < Re < 20$. It should be noted that the lower limit on Re does not extend to zero, because of the well-known Stokes paradox according to which there is no steady solution to Stokes flow past an infinitely long cylinder in an unbounded medium. Next, to account for finite ϕ, it is suggested that Re be evaluated based on an equivalent radius determined from

$$a_{eq} = \frac{2 \times \text{flow area}}{\text{wetted perimeter}} = a\frac{1 - \phi}{\phi}. \tag{33}$$

Thus, according to this recipe, the coefficient C is given by

$$C_{eq} = 0.623\left(\frac{1 - \phi}{\phi}\right)^{1/3}. \tag{34}$$

For $\phi = 0.05$, 0.3, and 0.6, the above expression predicts C equal to, respectively, 1.66, 0.83, and 0.54. In contrast, our calculations for small Re give C equal to 0.54, 0.94, and 1.88, respectively. Thus we conclude that the use of the equivalent radius concept may give quite an erroneous estimate of the effect of ϕ on the heat transfer coefficients for flow past cylinders in heat exchangers.

IV. AN APPROXIMATE RELATION

Since N in the limit of large Pe and K at small Re are governed by the stress distribution on the surface of the par-

Phys. Fluids, Vol. 9, No. 6, June 1997

W. Wang and A. S. Sangani   1537

TABLE V. A comparison of C estimated from (35) (C_{app}) with various known results (C_{ex}) for arrays of spheres. Dilute, sc, random, and fcc refer, respectively, to the case of isolated particle, simple cubic, face-centered cubic, and random packed arrays.

ϕ	Array	$\dfrac{F}{6\pi\mu Ua}$	C_{ex}	C_{app}
0	dilute	1	0.62	0.61
0.52	sc	42.1	1.29-1.46	1.41
0.62	random	113	1.82	1.77
0.74	fcc	438	2.83	2.41

ticles, it is useful to attempt to correlate the two. Our results for random arrays of cylinders may be satisfactorily correlated by means of a simple expression

$$C = (0.37 - 0.24\phi)(\phi K)^{-1/3}. \tag{35}$$

This correlation appears to be satisfactory even for the case of spherical particles as shown in Table V, where we have compared it with various known results. For spherical particles, the permeability is related to the average drag force and mean velocity by

$$\frac{1}{\phi K} = \frac{9}{2}\frac{F}{6\pi\mu Ua}. \tag{36}$$

For isolated particles, i.e., for $\phi \to 0$, (35) with $\phi K = 2/9$ yields $C = 0.61$, which is in very good agreement with the exact result $C = 0.6245 \ldots$.[6] As mentioned in the introduction, Sorensen and Stewart[2] determined C for simple cubic and face-centered cubic arrays at their maximum volume fractions of $\phi = 0.5236$ and 0.7405, respectively. For the case of simple cubic array, they evaluated C for two orientations of the mean flow: for $(0,0,1)$ and $(1,1,1)$ directions, the principal lattice directions being along the three coordinate axes. The corresponding values of C reported by these investigators are 1.29 and 1.46. The nondimensional drag force $F/(6\pi\mu Ua)$ for periodic arrays of spheres has been accurately evaluated by Zick and Homsy[22] and Sangani and Acrivos.[23] Using their value of 42.1 for packed simple cubic arrays (35) and (36) yields $C = 1.41$ in very good agreement with the result obtained by Sorensen and Stewart for the $(1,1,1)$ direction. Next, we consider the face-centered cubic array with $\phi = 0.7405$ for which Sorensen and Stewart obtained $C = 2.83$. The mean flow in this calculation was along the $(0,0,1)$ direction which is oriented at 45° to a principal lattice direction $(0,1,1)$, of the array. As mentioned by these investigators their result for C agrees to within 2 per cent of the experimental value for C reported by Karabelas et al.[24] who conducted electrochemical measurements for a single active sphere in a packed face-centered cubic array. Using $F/(6\pi\mu Ua) = 438$ for this array, (35) and (36) yield $C = 2.41$ which agrees within about 20% with the exact value of 2.83. Finally, C for packed random arrays of spheres may be estimated from the mass transfer correlation of Wilson and Geankoplis,[25] according to which

$$N = \frac{0.69}{1-\phi}Pe^{1/3}. \tag{37}$$

The above correlation for dumped, packed beds of spheres is expected to apply for $Re < 55$, $Pe > 50$, and $0.25 < \phi < 0.65$. We shall use this correlation to obtain C for packed equal-size spheres with $\phi = 0.62$. The well-known Kozeny equation,

$$\frac{F}{6\pi\mu Ua} = 10\frac{\phi}{(1-\phi)^3}, \tag{38}$$

yields a nondimensional drag of approximately 113. This compares well with the results of numerical simulations by Mo and Sangani[17] and with careful experimental measurements of the same for monodispersed packed beds by Philipse and Pathmamanoharan.[26] Substituting this value in (35) and (36), we obtain $C = 1.86$, which compares very well with $C = 1.77$ obtained from (37) with $\phi = 0.62$.

In summary we find that (35) appears to be remarkably accurate for the arrays of both cylinders and spheres for a wide range range of values of ϕ over which ϕK varies by three orders of magnitude.

ACKNOWLEDGMENTS

[1] J. P. Sorensen and W. E. Stewart, ''Computation of forced convection in slow flow through ducts and packed beds—III. Heat and mass transfer in a simple cubic array of spheres,'' Chem. Eng. Sci. **29**, 827 (1974).

[2] J. P. Sorensen and W. E. Stewart, ''Computation of forced convection in slow flow through ducts and packed beds—IV. Convective boundary layers in cubic arrays of spheres,'' Chem. Eng. Sci. **29**, 833 (1974).

[3] A. S. Sangani and A. Acrivos, ''Slow flow past periodic arrays of cylinders with application to heat transfer,'' Int. J. Mutliphase Flow **8**, 193 (1982).

[4] A. Acrivos, E. J. Hinch, and D. J. Jefferey, ''Heat transfer to a slowly moving fluid from a dilute fixed bed of heated sphere,'' J. Fluid Mech. **101**, 403 (1980).

[5] A. S. Sangani and C. Yao, ''Transport processes in random arrays of cylinders. II. Viscous flow,'' Phys. Fluids **31**, 2435 (1988).

[6] V. G. Levich, *Physicochemical Hydrodynamics* (Moscow, 1959).

[7] S. K. Friedlander, ''A note on transport to spheres in Stokes flow,'' J. Am. Inst. Chem. Eng. **7**, 347 (1961).

[8] N. A. Frankel and A. Acrivos, ''Heat and mass transfer from small spheres and cylinders freely suspended in shear flow,'' Phys. Fluids **11**, 1993 (1968).

[9] A. Acrivos, ''Heat transfer at high Peclet number from a small sphere freely rotating in a simple shear flow,'' J. Fluid Mech. **46**, 233 (1971).

[10] L. G. Leal, *Laminar Flow and Convective Transport Processes* (Butterworth-Heinemann, Washington, DC, 1992).

[11] The authors are grateful to Professor Koch for the scaling arguments presented here.

[12] R. E. Larson and J. J. L. Higdon, ''Microscopic flow near the surface of two-dimensional porous media. Part 2. Transverse flow,'' J. Fluid Mech. **178**, 119 (1987).

[13] C. K. Ghaddar, ''On the permeability of unidirectional fibrous media: A parallel computational approach,'' Phys. Fluids **7**, 2563 (1995).

[14] A. S. Sangani and G. Mo, ''Inclusion of lubrication forces in dynamic simulations,'' Phys. Fluids **6**, 1653 (1994).

[15] D. L. Koch and A. J. C. Ladd, ''Moderate Reynolds number flow through periodic and random arrays of aligned cylinders,'' to appear in J. Fluid Mech.

[16] T. L. Dodd, D. A. Hammer, A. S. Sangani, and D. L. Koch, ''Numerical simulations of the effect of hydrodynamic interactions on diffusivities of integral membrane proteins,'' J. Fluid Mech. **293**, 147 (1995).

W. Wang and A. S. Sangani

[17] G. Mo and A. S. Sangani, ''A method for computing Stokes flow interactions among spherical objects and its application to suspensions of drops and porous particles,'' Phys. Fluids **6**, 1637 (1994).

[18] D. G. Chae, F. H. Ree, and T. Ree, ''Radial distribution functions and equation of state of the hard disk fluid,'' J. Chem. Phys. **50**, 1581 (1969).

[19] X. Tkatschaw and A. S. Sangani (private communication).

[20] A. S. Sangani and G. Mo, ''Elastic interactions in particulate composites with perfect as well as imperfect interfaces ,'' to appear in J. Mech. Phys. Solids.

[21] J. R. Welty, C. E. Wicks, and R. E. Wilson, *Fundamentals of Momentum, Heat, and Mass Transfer* (Wiley, New York, 1984).

[22] A. Zick and G. M. Homsy, ''Stokes flow through periodic arrays of spheres,'' J. Fluid Mech. **115**, 13 (1982).

[23] A. S. Sangani and A. Acrivos, ''Slow flow through a periodic array of spheres,'' Int. J. Multiphase Flow **8**, 343 (1982).

[24] A. J. Karabelas, T. H. Wegner, and T. J. Hanratty, ''Use of asymptotic relations to correlate mass transfer data in packed bed,'' Chem. Eng. Sci. **26**, 1581 (1971).

[25] E. J. Wilson and C. J. Geankoplis, ''Liquid mass transfer at very low Reynolds number in packed beds,'' Ind. Eng. Chem. Fund. **59**, 9 (1966).

[26] A. P. Philipse and C. Pathmamanoharan, ''Liquid permeation (and sedimentation) of dense colloidal hard-sphere packings,'' J. Colloid Interface Sci. **159**, 96 (1993).